



Structural and Magnetic Tuning from Field-Induced Single-Ion Magnet to Single-Chain Magnet by Anions

Journal:	<i>Inorganic Chemistry Frontiers</i>
Manuscript ID:	QI-RES-05-2015-000089.R1
Article Type:	Research article
Date Submitted by the Author:	29-Jun-2015
Complete List of Authors:	Shao, Dong; Nanjing University, Chemistry Zhao, Xinhua; Nanjing University, Chemistry Zhang, Shaoliang; Nanjing University, Chemistry Wu, Dongqing; Nanjing University, Chemistry Wei, Xiaoqin; Nanjing University, Chemistry Wang, Xin-Yi; Nanjing University, Chemistry



Structural and Magnetic Tuning from Field-Induced Single-Ion Magnet to Single-Chain Magnet by Anions

Dong Shao, Xin-Hua Zhao, Shao-Liang Zhang, Dong-Qing Wu, Xiao-Qin Wei and Xin-Yi Wang*

Received 00th January 2015,
Accepted 00th January 2015

DOI: 10.1039/x0xx00000x

www.rsc.org/

We herein reported the syntheses, crystal structures, and magnetic properties of two complexes based on the anisotropic pentagonal bipyramidal Fe^{II} starting material [Fe(L_{N3O2})]²⁺, namely [Fe(L_{N3O2})(H₂O)₂][MQ]₂·H₂O (**1**) and [Fe(L_{N3O2})(CN)][ABSA]·3H₂O (**2**) (L_{N3O2} = 2,13-dimethyl-6,9-dioxo-3,12,18-triazabicyclo[12.3.1]octadeca-1(18),2,12,14,16-pentaene; MQ⁻ = methyl orange anion; ABSA⁻ = 4-aminoazobenzene-4'-sulfonic anion). Compound **1** is a mononuclear material where the [Fe(L_{N3O2})(H₂O)₂]²⁺ cations form a one-dimensional (1D) chain by the hydrogen bonds between the bulky MQ⁻ anions and the coordinated water molecules. With a slightly different anion ABSA⁻, cyano-bridged Fe^{II} chain is formed for compound **2**. This chain has a similar structure as that in our recently reported compound [Fe(L_{N5})(CN)][BF₄] (*Chem. Commun.* 2015, **51**, 4360). However, compared with the reported result where the chains interact with each other through the π···π interactions, the chains in **2** are well isolated by the bulky ABSA⁻ anions with the shortest interchain Fe···Fe distances around 12.0 Å. Magnetic investigation on **1** reveals the easy-axis magnetic anisotropy of the mononuclear Fe^{II} centre (zero-field splitting parameter $D = -3.7 \text{ cm}^{-1}$), which leads to the field-induced slow magnetic relaxation. For compound **2**, the Fe²⁺ spins are antiferromagnetically coupled through the cyano bridges with a coupling constant of $J = -4.13(2) \text{ cm}^{-1}$ with the Hamiltonian $H = -JS_i \cdot S_{i+1}$. Ac magnetic measurements revealed the pure single-chain magnet (SCM) behaviour of these isolated chains with an effective energy barrier of 26.1(5) K. This system represents a good example showing that the structures and magnetic properties, such as field-induced single-ion magnets, SCMs, and SCM-based magnets, can be selectively prepared by anion modification.

Introduction

Molecular nanomagnets of slow magnetic relaxation below their blocking temperatures, such as the single-molecule magnets (SMMs), single-ion magnets (SIMs) and single-chain magnets (SCMs), are of great interest in the field of molecular magnetism.¹ Among them, SCMs received great attention ever since its first observation in a Co^{II}-nitroxide radical chain in 2001.^{2,3} Theoretically, because of the additional energy component known as correlation energy (Δ_c) stemming from the exchange coupling (J) between the spin centres along the chain, SCMs might display higher relaxation barriers than their counterpart single-molecule magnets (SMMs).⁴⁻¹⁰

For the construction of SCMs, the magnetic anisotropy of spin unit, intrachain exchange interaction and interchain interaction are three most important factors. However, compared with the former two ingredients which are the stronger the better, the interchain interactions require more careful consideration. Initially, it was believed that negligible interchain coupling is necessary to prevent the three-

dimensional magnetic ordering and to achieve the SCM behaviour. Later, it was found that SCM behaviour can be retained in the antiferromagnetic (AF)^{4a} or ferromagnetic (F)^{4b,c} ordered phases. By taking advantage of the magnetic ordering, new types of high temperature SCM-based magnets can be achieved.⁵ Following the experimental and theoretical work of Coulon and Clérac et al,^{4a,5} a number of SCM-based antiferromagnets have been reported.⁶⁻⁸ These SCM-based antiferromagnets suggest a possible strategy for high temperature SCM-based magnets.

Synthetically, the magnetic anisotropy and intrachain magnetic coupling can be manipulated by using anisotropic spin carriers⁴⁻¹⁰ and bridging ligands as efficient magnetic couplers such as the cyanide,^{6,7a,c,h} radicals^{2a,4b,10} or other short bridges.^{7b-h,8} On the other hand, the design and control of the interchain interaction seems rather difficult. Several parameters can be manipulated to finely tune the interchain distances (and thus the interchain magnetic coupling), such as the counter ions or chelating ligands of different size,^{3d,9a,10b,g} different bisonodentate bridging ligands of different lengths,^{9b-d} interchain hydrogen bonds^{9e} and interchain π-π interactions.^{6,7b} For now, it still remains a synthetic challenge for the chemists to tune the interchain distances and also the magnetic property at will for a specific chain compound. As an illustrative example, Clérac et al reported the compound [Mn(3,5-Cl₂salmten)Ni(pao)₂(phen)][PF₆] in 2010,⁵ where the

*State Key Laboratory of Coordination Chemistry, Collaborative Innovation Center of Advanced Microstructures, School of Chemistry and Chemical Engineering, Nanjing University, Nanjing, 210093, China †
E-mail: wangxy66@nju.edu.cn
Fax: +86-25-83314502

anion can be replaced from PF_6^- to the bulky BPh_4^- , leading to the modification of the magnetic property from SCM-based antiferromagnet to the pure SCM.

Very recently, using an anisotropic pentagonal bipyramidal Fe^{II} starting material, we prepared a cyano-bridged homospin compound $[\text{Fe}(\text{L}_{\text{N}_5})(\text{CN})][\text{BF}_4]$, which exhibits the rare coexistence of spin-canting, AF ordering, metamagnetism and SCM behaviour.⁶ Its strong magnetic anisotropy arises from the pentagonal bipyramidal Fe^{II} center, as has been shown by Sutter, Mallah and Gao et al in the field-induced SIMs,¹¹ and cyano-bridged SMM^{12a} and SCM compounds.^{12b} Because of the small size of the BF_4^- anion, the chains in $[\text{Fe}(\text{L}_{\text{N}_5})(\text{CN})][\text{BF}_4]$ are not well isolated and interact to each other by π - π interactions. These weak interactions are believed to be responsible for the weak interchain magnetic coupling and the long-range magnetic ordering. Since this compound is synthesized in the presence of excessive BF_4^- anions, this system provides a good opportunity to tune the interchain distances with anions of difference sizes. Along this line, we performed the reaction using a similar starting material $[\text{Fe}(\text{L}_{\text{N}_{302}})(\text{CN})_2]$ with the bulky anions MQ^- and ABSA^- ($\text{L}_{\text{N}_{302}} = 2,13$ -dimethyl-6,9-dioxo-3,12,18-triazabicyclo[12.3.1]octadeca-1(18),2,12,14,16-pentaene; MQ^- = methyl orange anion; ABSA^- = 4-aminoazobenzene-4'-sulfonic anion, Fig. 1). Interestingly, a mononuclear Fe^{II} compound $[\text{Fe}(\text{L}_{\text{N}_{302}})(\text{H}_2\text{O})_2][\text{MQ}]_2 \cdot \text{H}_2\text{O}$ (**1**) and a cyano-bridged 1D chain compound $[\text{Fe}(\text{L}_{\text{N}_{302}})(\text{CN})][\text{ABSA}] \cdot 3\text{H}_2\text{O}$ (**2**) were obtained. The chains in **2** are well isolated by the large ABSA^- anions. Magnetic studies revealed that **1** exhibits field-induced slow magnetic relaxation and **2** is a pure SCM with an effective energy barrier of 26.1(5) K.

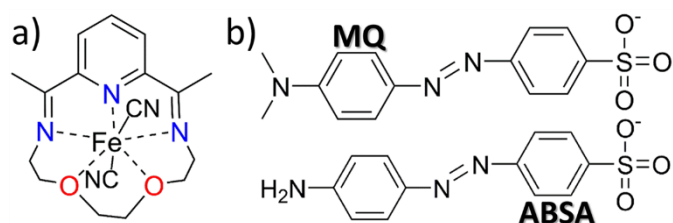


Fig. 1 View of the structures of the $[\text{Fe}(\text{L}_{\text{N}_{302}})(\text{CN})_2]$ starting material (a) and the bulky anions MQ^- and ABSA^- (b).

Experimental Section

Physical Measurements

Infrared spectra data were measured on KBr pellets using a Nexus 870 FT-IR spectrometer in the 4000-400 cm^{-1} range. Elemental analyses of C, H, and N were performed at an Elementar Vario MICRO analyzer. Powder X-ray diffraction data (PXRD) were recorded at 298 K on a Bruker D8 Advance diffractometer with $\text{Cu K}\alpha$ X-ray source operated at 40 kV and 40 mA. Thermal gravimetric analysis (TGA) was measured on a STA 449 F3 Jupiter analyzer in the temperature range of 40-800 $^{\circ}\text{C}$. Magnetic measurements from 2 to 300 K with dc field up to 70 kOe were performed using a Quantum Design SQUID VSM magnetometer on the grounded powders from the single

crystals of the compounds. Alternative current (ac) magnetic susceptibility data were collected in a zero dc field or 2000 Oe dc field in the temperature range of 2.0-10 K, under an ac field of 2 Oe, oscillating at frequencies in the range of 1-950 Hz. All magnetic data were corrected for the diamagnetism of the sample holder and of the diamagnetic contribution of the sample ($-0.5 \times 10^{-6} \times$ molecular weight).

Materials and Synthesis

All reagents were obtained from commercially available sources and used as received unless otherwise noted. Solvents were distilled before use under a N_2 atmosphere. The synthesis and crystal growth procedures were performed under a N_2 atmosphere using Schlenk techniques or in a N_2 atmosphere glovebox. $[\text{Fe}(\text{L}_{\text{N}_{302}})(\text{CN})_2]$ were synthesized according to the literature method.¹³

Caution!

Cyanides are highly toxic and they should be handled in small quantities with care.

$[\text{Fe}(\text{L}_{\text{N}_{302}})(\text{H}_2\text{O})_2][\text{MQ}]_2 \cdot \text{H}_2\text{O}$ (1): A solution of methyl orange (NaMQ , 40 mg, 0.12 mmol) in 1 mL of water was added to a solution of $[\text{Fe}(\text{L}_{\text{N}_{302}})(\text{CN})_2]$ (25 mg, 0.05 mmol) in 6 mL of methanol under nitrogen atmosphere. The dark violet solution was filtrated to a vial and was then kept in the dark place for one week. Dark blue rhombus single crystals formed after slow evaporation. The crystals were filtered and washed with methanol. Yield: ~ 27 mg, 54% based on $[\text{Fe}(\text{L}_{\text{N}_{302}})(\text{CN})_2]$. The crystals are quite stable in the air. Elemental analysis (%) for $\text{C}_{43}\text{H}_{55}\text{FeN}_9\text{O}_{11}\text{S}_2$: C, 51.96; H, 5.58; N, 12.68. Found: C, 51.89, H, 5.60; N, 12.58. IR (KBr, cm^{-1}): 3362(vs), 2921(s), 2887(s), 1606(vs), 1520(s), 1421(s), 1370(vs), 1221(s), 1115(vs), 1031(vs), 1005(s), 847(s), 818(s), 693(s), 619 (s).

$[\text{Fe}(\text{L}_{\text{N}_{302}})(\text{CN})][\text{ABSA}] \cdot 3\text{H}_2\text{O}$ (2): By replacing Methyl Orange with 4-Aminoazobenzene-4'-sulfonic acid sodium salt (NaABSA), compound **2** was also obtained as black block crystals according to the same synthetic procedure as compound **1**. Yield: ~ 18 mg, 52% based on $[\text{Fe}(\text{L}_{\text{N}_{302}})(\text{CN})_2]$. The crystals are also quite stable in the air. Elemental analysis (%) for $\text{C}_{28}\text{H}_{37}\text{FeN}_7\text{O}_8\text{S}$: C, 48.91; H, 5.42; N, 14.26. Found: C, 48.99, H, 5.35; N, 14.28. IR (KBr, cm^{-1}): 3337 (vs), 2925 (vs), 2881(s), 2123(s), 1635(vs), 1596 (vs), 1504(s), 1420(s), 1219(vs), 1194(vs), 1116 (vs), 1030 (vs), 711(s), 627 (s).

X-ray Crystallography

Single crystal X-ray crystallographic data were collected on a Bruker APEX II diffractometer with a CCD area detector ($\text{Mo-K}\alpha$ radiation, $\lambda = 0.71073 \text{ \AA}$) at room temperature. The APEXII program was used to determine the unit cell parameters and for data collection. The data were integrated and corrected for Lorentz and polarization effects using SAINT.¹⁴ Absorption corrections were applied with SADABS.¹⁵ The structures were solved by direct methods and refined by full-matrix least-squares method on F^2 using the SHELXTL crystallographic software package.¹⁶ All the non-hydrogen atoms were refined anisotropically. Hydrogen atoms of the organic ligands were

refined as riding on the corresponding non-hydrogen atoms. Additional details of the data collections and structural refinement parameters are provided in Table 1. Selected bond lengths and angles of **1** and **2** are listed in Table S1 (Supporting Information).

Table 1. Crystallographic data and structure refinement parameters for complexes **1** and **2**.

	1	2
Formula	C ₄₃ H ₅₅ FeN ₉ O ₁₁ S ₂	C ₂₈ H ₃₇ FeN ₇ O ₈ S
Formula weight [g mol ⁻¹]	993.93	687.56
Crystal size [mm ³]	0.56 × 0.15 × 0.08	0.63 × 0.22 × 0.15
Crystal system	triclinic	monoclinic
Space group	<i>P</i> $\bar{1}$	<i>P</i> 2 ₁ / <i>c</i>
<i>a</i> [Å]	8.5081(2)	12.7854(1)
<i>b</i> [Å]	11.345(2)	10.5316(9)
<i>c</i> [Å]	24.713(5)	24.534(2)
α [°]	76.947(3)	90
β [°]	87.749(3)	97.8160(1)
γ [°]	85.552(3)	90
<i>V</i> [Å ³]	2316.3(8)	3272.8(5)
<i>Z</i>	2	4
<i>T</i> [K]	293(2)	293(2)
ρ_{calcd} [g cm ⁻³]	1.425	1.395
$\mu(\text{Mo-K}\alpha)$ [mm ⁻¹]	0.485	0.582
<i>F</i> (000)	1044	1440
<i>R</i> _{int}	0.0209	0.0532
<i>R</i> ₁ ^a / <i>wR</i> ₂ ^b (<i>I</i> > 2 σ (<i>I</i>))	0.0688 / 0.1836	0.0488 / 0.1272
<i>R</i> ₁ / <i>wR</i> ₂ (all data)	0.0846 / 0.1959	0.0565 / 0.1381
GOF on <i>F</i> ²	1.010	1.062

$$^a R_1 = \sum |F_o| - |F_c| / \sum |F_o|, \quad ^b wR_2 = \left\{ \sum [w(F_o^2 - F_c^2)^2] / \sum [w(F_o^2)^2] \right\}^{1/2}$$

Results and Discussion

Synthesis

As reported for the synthesis of compound [Fe(L_{N5})(CN)][BF₄], compounds **1** and **2** were prepared by recrystallization of the [Fe(L_{N3O2})(CN)₂] starting material in the presence of the bulky anions. The stability of the [Fe(L_{N3O2})(CN)₂] compound in solution seems even lower than that of [Fe(L_{N5})(CN)₂]. Both of the CN groups were replaced by the water molecules to form the isolated mononuclear compound **1**; and one of the CN groups were disassociated to from the 1D compound **2** as observed in [Fe(L_{N5})(CN)][BF₄].⁶ Although the difference between the MA⁻ and ABSA⁻ anions is very minor (Fig. 1), attempts to isolate the 1D structure using the MA⁻ anion failed. The purity of **1** and **2** was confirmed by the powder XRD spectra and the elemental analysis (Fig. S1, S2, ESI[†]). Thermal gravimetric analysis (TGA) on **2** shows 8.3 % weight loss in the temperature range of 40–110 °C, corresponding to the removal of three crystallized water molecules (calc. 7.9 %, Fig. S3, ESI[†]).

Crystal Structure Descriptions

Single-crystal X-ray diffraction analyses for **1** and **2** reveal that **1** crystallized in the triclinic space group *P* $\bar{1}$ and **2** in the

monoclinic space group *P*2₁/*c* (Table 1). The asymmetric unit of **1** contains a mononuclear Fe^{II} cation chelated by one L_{N3O2} ligand, two water molecules axially coordinated to Fe²⁺, two MQ⁻ anions for the charge balance, and one lattice water molecule (Fig. 2a, Table S1, ESI[†]). Of the two MQ⁻ anions, one of them contains the disordered N=N group. Each Fe^{II} centre resides in a N₃O₄ pentagonal bipyramid environment with a continuous shape measure (CSHM)¹⁷ calculated to be 0.208 relative to the ideal *D*_{5h} geometry. The O_{axial}-Fe-O_{axial} angle of 174.7(8)^o is close to linearity and the axial bonds (Fe-O3 = 2.142(3) Å and Fe-O4 = 2.125(3) Å) are slightly shorter than the average bonds of 2.212(6) Å in the equatorial plane. Hydrogen bonds were found between the coordinated water molecules and the oxygen atoms from the SO₃ groups of the MQ⁻ anion (O3...O6 = 2.740, O3...O9 = 2.740 Å, O4...O7 = 2.733, O4...O11 = 2.684). Bridged by these effective hydrogen bond interactions, a 1D supramolecular chain structure is formed along the *a* axis (Fig. 2b). These chains were further connected by the hydrogen bonds between the SO₃ groups and the lattice water molecules (O5...O8 = 2.812, O5...O10 = 3.049 Å), forming a 2D layer along the *ab* plane, which is further separated by the bulky MQ⁻ anions along the *c* direction (Fig. S4, ESI[†]). The shortest Fe...Fe distance in **1** is 7.85 Å.

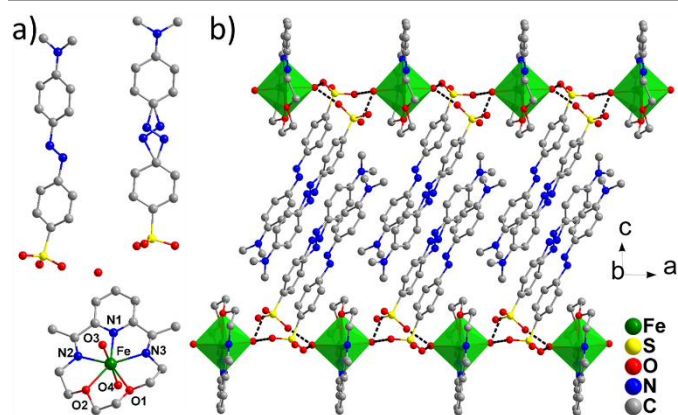


Fig. 2 View of the asymmetric unit (a) and the hydrogen bonded 1D chain (b) of **1**. Hydrogen atoms were omitted for clarity.

The structure of **2** is very similar to that of the reported [Fe(L_{N5})(CN)][BF₄] compound, with 1D cyano-bridged Fe^{II} chain separated by the bulky ABSA⁻ anions (Fig. 3c, S5, ESI[†]). The Fe^{II} centre is also in a pentagonal bipyramid geometry with a N₄O₂C₁ coordination environment and the CSHM parameter is 0.295 to an ideal *D*_{5h} symmetry (Fig. 3a). Bridged by the cyano groups, regular chains along the *b* axis are formed with the shortest Fe-Fe distance of 5.30 Å (Fig. 3b). As in [Fe(L_{N5})(CN)][BF₄], the pseudo 5-fold axis the Fe^{II} centre (C_{cyano}-Fe-N_{cyano} axis) is tilted away from the *b* axis with an angle of ~ 6° (Fig. 3b). The ABSA⁻ counter anions lie in between the chains and form abundant hydrogen bonds among themselves (NH₂-SO₃) and between the lattice water molecules (Fig. S6, ESI[†]). Interestingly, these bulky organic anions efficiently separate the 1D chains away from each other and prevent any supramolecular interactions between the chains, such as the π - π interactions found in [Fe(L_{N5})(CN)][BF₄]. As a result, the

shortest interchain Fe...Fe distance increases to 12.0 Å along the *a* direction and 12.8 Å along the *c* direction (Fig. 3c), compared to the 9.73 Å in [Fe(L_{NS})(CN)][BF₄]. The increased isolation of the 1D chains efficiently decreases the interchain magnetic interaction and leads to the pure SCM behaviour in **2**, as can be seen from the magnetic measurements below.

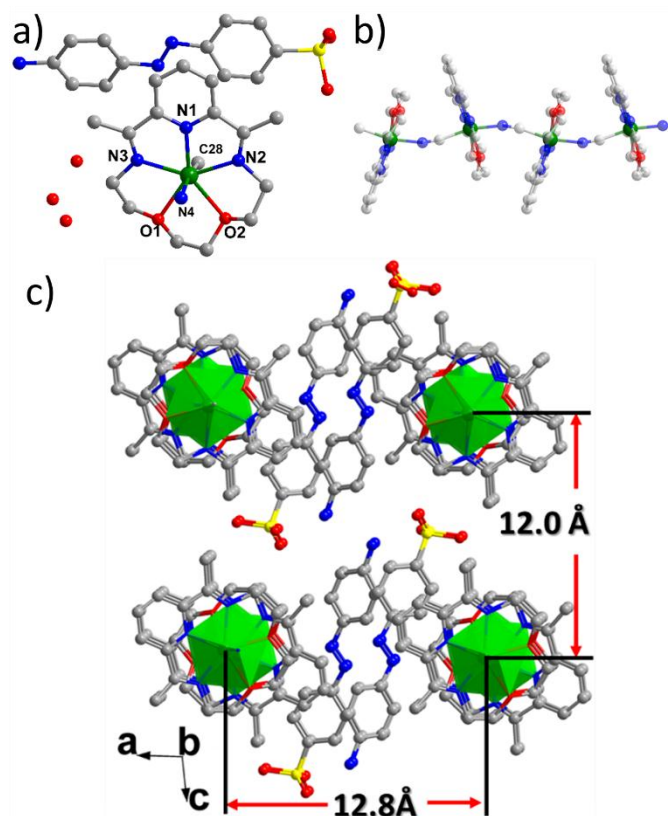


Fig. 3 View of the asymmetric unit (a), the chain structure along the *b* axis (b), and the packing diagram (c) of **2**.

Magnetic Properties

Temperature dependent magnetic susceptibility data of **1** and **2** in the temperature range of 2–300 K were measured under a dc field of 1 kOe. The $\chi_M T$ value at 300 K for **1** was 3.70 cm³ mol⁻¹ K (Fig. 4a), which is larger than the spin-only value of 3.00 cm³ mol⁻¹ K for a high-spin Fe^{II} ion (*S* = 2, *g* = 2), indicating the magnetic anisotropy of Fe^{II} in a near *D*_{5h} ligand field.^{11–12} Upon cooling, the $\chi_M T$ values decreased monotonously down to a minimum of 2.50 cm³ mol⁻¹ K at 2 K. The field-dependent magnetization measured at 2 K shows a typical paramagnetic behaviour with the largest *M* value of 3.4 μ_B at 70 kOe (Fig. 4a, insert), which is less than the saturation value of 4 μ_B for a spin-only Fe^{II} with *S* = 2. The $\chi_M(T)$ and *M*(*H*) curves of **1** can be simultaneously fitted with the following Hamiltonian by the software PHI¹⁸:

$$H = D[S_z^2 - S(S+1)/3] + E(S_x^2 - S_y^2) + \mu_B \mathbf{g} \cdot \mathbf{S} \cdot \mathbf{B}$$

The best fit gives *D* = -3.7 cm⁻¹, *E* = 0.02 cm⁻¹, *g_x* = *g_y* = 2.32 and *g_z* = 1.92. Also, the magnetic anisotropy of the Fe^{II} ion in the pentagonal bipyramid geometry was further confirmed by the reduced magnetization of **1** measured at low temperatures. As can be seen in Fig. 4b, these magnetization plots exhibit

significant separation between the isofield curves and can be well fitted using Anisoft 2.0,¹⁹ giving *D* = -3.7 cm⁻¹, *E* = 0.02 cm⁻¹, and *g* = 2.21. These values agree very well with the parameters obtained above. Although the *D* value obtained for **1** is significantly smaller than that of the reported compounds of the similar pentagonal bipyramid geometry (around -10 to -16 cm⁻¹) by Sutter et al.,^{11a,12} the negative *D* value indicates the easy-axis magnetic anisotropy and suggests the possibility of observing slow magnetic relaxation behaviour. Indeed, Fe^{II} compounds with pentagonal bipyramid geometry can exhibit very strong magnetic anisotropy with large negative *D* value, supported by theoretical and high-field EPR studies.^{11, 20} A recent result illustrates that not only the oxo-ligands from the axial coordination sites but also the supramolecular organization have a strong impact on the magnetic properties, including the anisotropy parameter *D*.¹¹

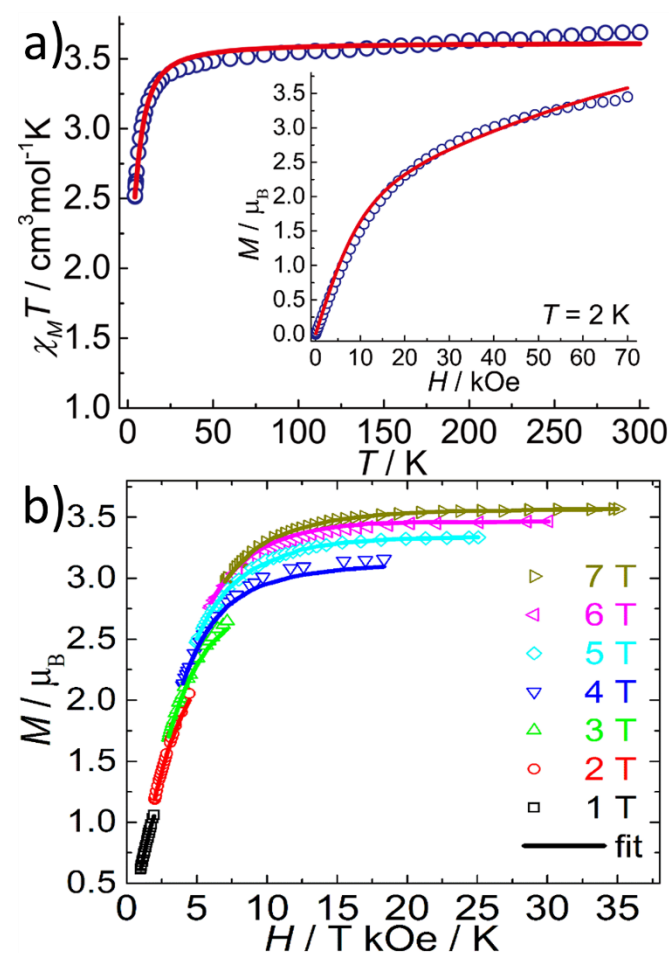


Fig. 4 a) Temperature dependent magnetic susceptibility for **1** measured at 1 kOe. Inset: field dependent magnetization curve at 2 K for **1**. The red lines represent the best fits by PHI; b) Reduced magnetization data for **1** collected under various applied dc fields. The lines represent the best fit by Anisoft 2.0.

Temperature dependent ac susceptibility measurements of **1** have been carried out under a zero or 2 kOe dc field. Although no out-of-phase signals were detected under zero dc field, frequency dependent χ'' signals were observed under 2 kOe dc field, indicating the field-induced slow magnetic relaxation behaviour of **1** (Fig. S7, ESI[†]). However, no peaks

were observed down to 2 K, in accordance with the small energy barrier of **1** due to the small D value.

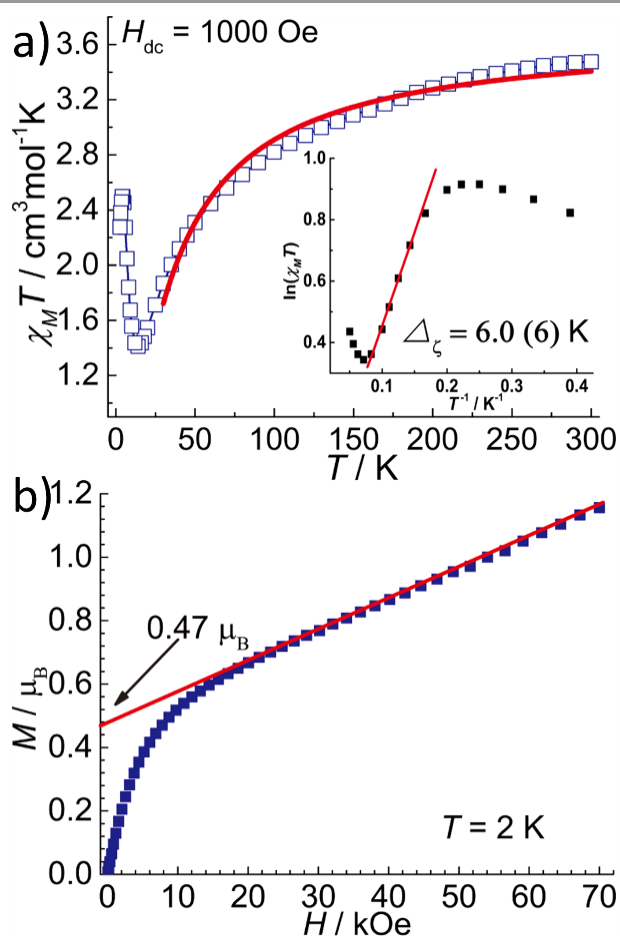


Fig. 5 a) Temperature dependent magnetic susceptibility of **2** measured at 1 kOe. Inset: $\ln(\chi_M T)$ vs $1/T$ plot; b) Field dependent magnetization curve for **2**.

As compound **2** has the very similar 1D chain structure as $[\text{Fe}(\text{L}_{\text{N5}})(\text{CN})][\text{BF}_4]$, its magnetic property is also very similar. First of all, the plot of $\chi_M T$ versus T is indicative of spin canting in an antiferromagnetic array (Fig. 5a).^{6,9e,21} Upon cooling, the $\chi_M T$ value decreased gradually from the room temperature value of $3.47 \text{ cm}^3 \text{ mol}^{-1} \text{ K}$ to a minimum of $1.41 \text{ cm}^3 \text{ mol}^{-1} \text{ K}$ at 14 K. Below 14 K, the $\chi_M T$ value increased sharply to a maximum of $2.49 \text{ cm}^3 \text{ mol}^{-1} \text{ K}$ at 4 K, and then decreased down to 2 K. Curie-Weiss fit of the data above 50 K gave a Curie constant of $3.92 \text{ cm}^3 \text{ mol}^{-1} \text{ K}$ and a negative Weiss constant of -39.6 K (Fig. S8, ESI[†]). The large and negative Weiss constant indicates the dominant antiferromagnetic interaction between the Fe^{II} centres, although it might also partly come from the spin-orbit coupling. The intrachain AF interaction was also estimated to be $J = -4.13 (2) \text{ cm}^{-1}$ ($g = 2.13 (3)$) by fitting the susceptibility data above 30 K using the same Fisher model ($H = -J \sum_{\text{Si-Si}+1}$) as we have previously employed for the compound $[\text{Fe}(\text{L}_{\text{N5}})(\text{CN})][\text{BF}_4]$.⁶ The intrachain magnetic interaction is almost the same as that for the $[\text{Fe}(\text{L}_{\text{N5}})(\text{CN})][\text{BF}_4]$, in consistent with their similar 1D structures. Thus, the different magnetic behaviour at low temperature (vide post) can be

mainly ascribed to the different interchain magnetic interaction.

The field dependent magnetization of **2** was measured at 2 K. As displayed in Fig. 5b, the magnetization increases quickly to $0.66 \mu_B$ at 20 kOe and then increases linearly up to $1.15 \mu_B$ at 70 kOe, which is far from the saturation value of $4 \mu_B$ for a high spin Fe^{II} with $S = 2$. This magnetization curve is similar to that of $[\text{Fe}(\text{L}_{\text{N5}})(\text{CN})][\text{BF}_4]$ and suggests the spin canting of the Fe^{II} spins, although the strong magnetic anisotropy might also play a role. The canting angle was estimated as 7.5° from the magnetization value of $0.47 \mu_B$ obtained by extrapolating the $M(H)$ curve in the high field region down to zero. Importantly, at low field region of the $M(H)$ curve, there is no S-shaped transition, ruling out the metamagnetic transition found for $[\text{Fe}(\text{L}_{\text{N5}})(\text{CN})][\text{BF}_4]$.⁶ This should originate from the weaker interchain magnetic coupling in **2**.

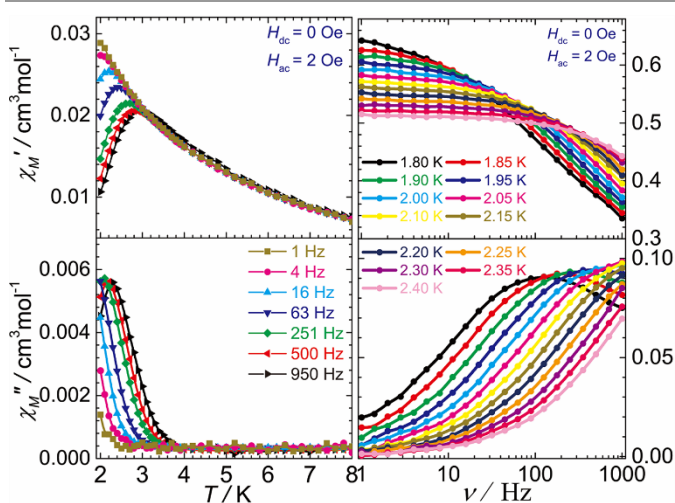


Fig. 6 Variable-temperature (a) and variable-frequency (b) ac magnetic susceptibility data for **2** measured in a zero dc field.

Because of the similar 1D structure and weaker interchain magnetic coupling, **2** should behave as a pure SCM, as confirmed by the ac susceptibility measurements performed under a zero dc field. As depicted in Fig. 6a, both the in-phase and out-of-phase temperature dependent ac signals were found to be strongly frequency dependent below 4 K, reflecting the slow magnetic relaxation. The Mydosh parameter $\varphi = (\Delta T_p / T_p) / (\Delta \log f)$, where T_p is the temperature of the peaks in χ' and f is the frequency, was found to be 0.3, which falls in the range ($0.1 < \varphi < 0.3$) expected for a superparamagnetic system.²² Most importantly, the frequency-independent peak at 5.4 K observed in $[\text{Fe}(\text{L}_{\text{N5}})(\text{CN})][\text{BF}_4]$ disappeared in the ac data of **2**, even under a zero dc field. Furthermore, variable-frequency ac susceptibility data collected from 1.8–2.4 K are also highly temperature dependent (Fig. 6b). The resulting Cole–Cole plots below 2.1 K can be fitted using a generalized Debye model²³ (Fig. 7a) with the parameter α in the range of 0.38–0.44 (Table S2), which suggests a moderate distribution of the relaxation time of **2**.²⁴ Fitting the relaxation time data to the Arrhenius equation $\tau = \tau_0 \exp(\Delta_\tau / T)$ gives the effective energy barrier $\Delta_\tau = 26.1(5) \text{ K}$ with the pre-exponential factor $\tau_0 = 8.3(6) \times 10^{-10} \text{ s}$ (Fig. 7b).

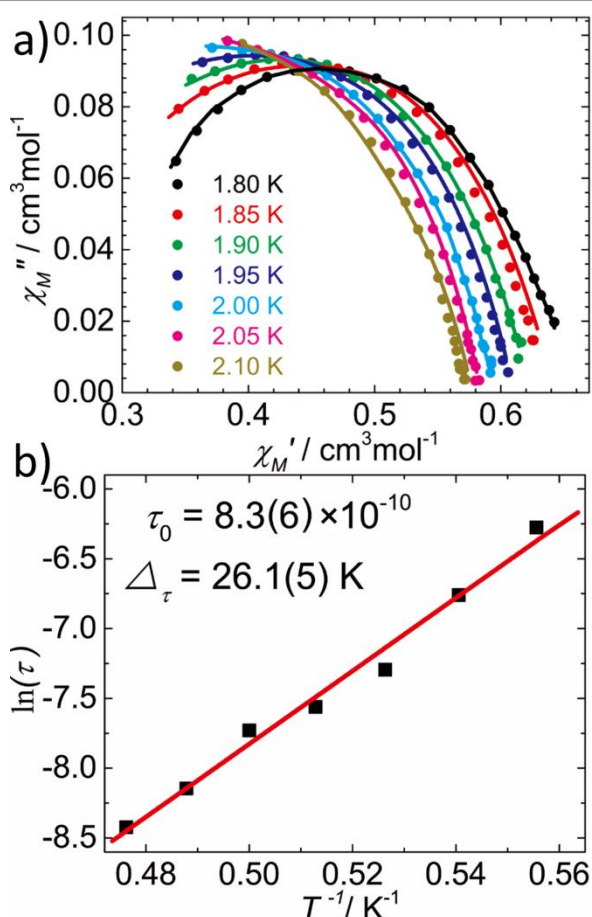


Fig. 7 a) Cole-Cole plots of **2** from 1.8 to 2.1 K. Solid lines represent the best fits to the experimental data according to the generalized Debye model; b) Arrhenius plot of the relaxation times.

For an anisotropic Heisenberg or Ising-like 1D system, it is well known that the $\chi_M T$ value is proportional to the correlation length (ξ) and increases exponentially with decreasing temperature, following the equation $\chi_M T = C_{\text{eff}} \exp(\Delta_\xi/T)$. The C_{eff} is the effective Curie constant and Δ_ξ gives an estimation of the intrachain exchange energy needed to create a domain wall within the chain. The resulting $\ln(\chi_M T)$ versus $1/T$ plot of **2** features a linear region in the temperature range of 6–12 K, yielding $C_{\text{eff}} = 0.85 \text{ cm}^3 \text{ mol}^{-1} \text{ K}$ and $\Delta_\xi = 6.06 \text{ K}$ (Fig. 5a). As the relaxation time of **2** used to estimate the effective energy barrier Δ_τ was determined at very low temperature (below 3 K), the slow relaxation is considered to be within the “finite-size chain” regime and the energy barrier should be given as $\Delta_\tau = \Delta_\xi + \Delta_A$. According to this relationship, the magnetic anisotropy energy Δ_A for the individual Fe^{2+} centres can be estimated as 20.0 K, which is almost equal to the value (20.1 K) in compound $[\text{Fe}(\text{L}_{\text{N}_5})(\text{CN})][\text{BF}_4]$. On the other hand, the correlation energy (Δ_ξ) in **2** is about one third of the value in $[\text{Fe}(\text{L}_{\text{N}_5})(\text{CN})][\text{BF}_4]$, and the blocking temperature of **2** is significantly lower than that of $[\text{Fe}(\text{L}_{\text{N}_5})(\text{CN})][\text{BF}_4]$ (for example, the peak temperature of the χ'' at 950 Hz is around 2.2 K for **2**, compared with 3.4 K for $[\text{Fe}(\text{L}_{\text{N}_5})(\text{CN})][\text{BF}_4]$). These observations indicate that the AF

ordering is of potential advantage for the properties of the SCM-based magnets.

Conclusions

In conclusion, reaction of a pentagonal bipyramidal Fe^{II} starting material of D_{5h} symmetry with excessive bulky anions results in two new magnetic materials of significant magnetic anisotropy and slow magnetic relaxation. Because of the terminal coordinated water molecules, compound **1** contains a mononuclear Fe^{II} centre, which is further connected by the hydrogen bonds to form extended structure. Easy-axis magnetic anisotropy with negative D value of about -3.7 cm^{-1} was obtained from the analysis of the dc magnetic data, which leads to the field-induced slow magnetic relaxation at low temperature. Interestingly, very minor change of the anion results in the 1D cyano-bridged chain structure of compound **2**. These 1D chains in **2** are well isolated by bulky anions and prevent any efficient interchain magnetic interaction. Because of the easy-axis magnetic anisotropy, AF magnetic coupling and spin canting, and the negligible interaction magnetic interaction, pure SCM behaviour with an effective energy barrier of 26.1(5) K is established in **2**. Both of these compounds and the formal reported system with a smaller anion clearly demonstrated the importance of the anions on the fine tuning of the structures and thus the magnetic properties of the resulting materials. Efforts to introduce functional anions and extend this chain architecture to other metal centres are under way.

Acknowledgements

We thank the Major State Basic Research Development Program (2013CB922102), NSFC (91022031, 21101093, 21471077). This work was also supported by a Project Funded by the Priority Academic Program Development of Jiangsu Higher Education Institutions.

Notes and references

‡ CCDC-1403677 (**1**) and 1403678 (**2**) contain the supplementary crystallographic data for this paper. These data can be obtained free of charge from the Cambridge Crystallographic Data Centre via www.ccdc.cam.ac.uk/data_request/cif.

†Electronic Supplementary Information (ESI) available: structure information in detail and additional magnetic data. For ESI and crystallographic data in CIFs or other electronic format see DOI: 10.1039/b000000x/.

- (a) D. Gatteschi, R. Sessoli and J. Villain, *Molecular Nanomagnets*, Oxford University Press, Oxford, 2006; (b) R. E. P. Winpenny, *Molecular Cluster Magnets*, World Scientific: London, 2012; (c) G. A. Craig and M. Murrell, *Chem. Soc. Rev.*, 2015, **44**, 2135.
- (a) A. Caneschi, D. Gatteschi, N. Lalioti, C. Sangregorio, R. Sessoli, G. Venturi, A. Vindigni, A. Rettori, M. G. Pini and M. A. Novak, *Angew. Chem., Int. Ed.*, 2001, **40**, 1760; (b) R.

- Clérac, H. Miyasaka, M. Yamashita and C. Coulon, *J. Am. Chem. Soc.*, 2002, **124**, 12837.
- 3 (a) S. Dhers, H. L. C. Feltham and S. Brooker, *Coord. Chem. Rev.*, 2015, **296**, 24; (b) W.-X. Zhang, R. Ishikawa, B. Breedlove and M. Yamashita, *RSC Advances*, 2013, **3**, 3772; (c) H.-L. Sun, Z.-M. Wang and S. Gao, *Coord. Chem. Rev.*, 2010, **254**, 1081; (d) H. Miyasaka, M. Julve, M. Yamashita and R. Clérac, *Inorg. Chem.*, 2009, **48**, 3420; (e) L. Bogani, A. Vindigni, R. Sessoli and D. Gatteschi, *J. Mater. Chem.*, 2008, **18**, 4750; (f) R. Lescouezec, L. M. Toma, J. Vaissermann, M. Verdagner, F. S. Delgado, C. Ruiz-Pérez, F. Lloret and M. Julve, *Coord. Chem. Rev.*, 2005, **249**, 2691.
- 4 (a) C. Coulon, R. Clérac, W. Wernsdorfer, T. Colin and H. Miyasaka, *Phys. Rev. Lett.*, 2009, **102**, 167204; (b) N. Ishii, Y. Okamura, S. Chiba, T. Nogami and T. Ishida, *J. Am. Chem. Soc.*, 2008, **130**, 24; (c) R. Sessoli, *Angew. Chem., Int. Ed.*, 2008, **47**, 5508.
- 5 H. Miyasaka, K. Takayama, A. S. Sayto, Furukawa, M. Yamashita and R. Clérac, *Chem.-Eur. J.*, 2010, **16**, 3656.
- 6 D. Shao, S.-L. Zhang, X.-H. Zhao and X.-Y. Wang, *Chem. Commun.*, 2015, **51**, 4360.
- 7 (a) Y.-Z. Zhang, H.-H. Zhao, E. Funck and K. R. Dunbar, *Angew. Chem., Int. Ed.*, 2015, **54**, 1; (b) L. Qin, Z. Zhang, Z.-P. Zheng, M. Speldrich, P. Kögerler, W. Xue, B.-Y. Wang, X.-M. Chen and Y.-Z. Zheng, *Dalton Trans.*, 2015, **44**, 1456; (c) I. Bhowmick, E. A. Hillard, P. Dechambenoit, C. Coulon, T. D. Harris and R. Clérac, *Chem. Commun.*, 2012, **48**, 9717; (d) X.-M. Liu, B.-Y. Wang, W. Xue, L.-H. Xie, W.-X. Zhang, X.-N. Cheng and X.-M. Chen, *Dalton Trans.*, 2012, **41**, 13741; (e) J. Boeckmann, M. Wriedt and C. Nather, *Chem. Eur. J.*, 2012, **18**, 5284; (f) J. H. Yoon, J. W. Lee, D. W. Ryu, S. W. Yoon, B. J. Suh, H. C. Kim and C. S. Hong, *Chem. - Eur. J.*, 2011, **17**, 3028; (g) C.-I. Yang, P.-H. Chuang and K.-L. Lu, *Chem. Commun.*, 2011, **47**, 4445; (h) T. Liu, Y.-J. Zhang, S. Kanegawa and O. Sato; *J. Am. Chem. Soc.*, 2010, **132**, 8250.
- 8 (a) X.-B. Li, G.-M. Zhuang, X. Wang, K. Wang and E.-Q. Gao, *Chem. Commun.*, 2013, **49**, 1814; (b) Y.-Q. Wang, Q. Yue, Y. Qi, K. Wang, Q. Sun and E.-Q. Gao, *Inorg. Chem.*, 2013, **52**, 4259; (c) X.-B. Li, G.-M. Zhuang, X. Wang, K. Wang and E.-Q. Gao, *Chem. Commun.*, 2013, **49**, 1814; (d) X.-M. Zhang, Y.-Q. Wang, K. Wang, E.-Q. Gao and C.-M. Liu, *Chem. Commun.*, 2011, **47**, 1815; (e) X.-M. Zhang, K. Wang, Y.-Q. Wang and E.-Q. Gao, *Dalton Trans.*, 2011, **40**, 12742; (f) Y.-Q. Wang, W.-W. Sun, Z.-D. Wang, Q.-X. Jia, E.-Q. Gao and Y. Song, *Chem. Commun.*, 2011, **47**, 6386.
- 9 (a) L. M. Toma, C. Ruiz-Pérez, F. Lloret and M. Julve, *Inorg. Chem.*, 2012, **51**, 1216; (b) L. M. Toma, C. Ruiz-Pérez, J. Pasán, W. Wernsdorfer, F. Lloret, and M. Julve, *J. Am. Chem. Soc.*, 2012, **134**, 15265; (c) Z.-X. Li, Y.-F. Zeng, H. Ma and X.-H. Bu, *Chem. Commun.*, 2010, **46**, 8540; (d) Y.-Z. Zheng, M.-L. Tong, W.-X. Zhang and X.-M. Chen, *Angew. Chem., Int. Ed.*, 2006, **45**, 6310; (e) W. X. Zhang, T. Shiga, H. Miyasaka, M. Yamashita, *J. Am. Chem. Soc.*, 2012, **134**, 6908.
- 10 (a) M. Zhu, J.-J. Wang, M. Yang, Y. Ma and L.-C. Li, *Dalton Trans.*, 2015, **44**, 9815; (b) Z.-X. Wang, X. Zhang, Y.-Z. Zhang, M.-X. Li, H.-H. Zhao, M. Andruh and K. R. Dunbar, *Angew. Chem., Int. Ed.*, 2014, **53**, 11567; (c) M. G. F. Vaz, P. M. Lahti, R. A. A. Cassaro and M. A. Novak, *Chem.-Eur. J.*, 2014, **20**, 1; (d) R. Ishikawa, K. Katoh, B. K. Breedlove and M. Yamashita, *Inorg. Chem.*, 2012, **51**, 9123; (e) K. Bernot, L. Bogani, R. Sessoli and D. Gatteschi, *Inorg. Chim. Acta*, 2007, **360**, 3807; (f) K. Bernot, L. Bogani, A. Caneschi, D. Gatteschi and R. Sessoli, *J. Am. Chem. Soc.*, 2006, **128**, 7947; (g) H. Miyasaka, T. Madanbashi, K. Sugimoto, Y. Nakazawa, W. Wernsdorfer, K. Sugiura, M. Yamashita, C. Coulon and R. Clérac, *Chem.-Eur. J.*, 2006, **12**, 7028; (h) N. Ishii, T. Ishida and T. Nogami, *Inorg. Chem.*, 2006, **45**, 3837; (i) L. Bogani, C. Sangregorio, R. Sessoli and D. Gatteschi, *Angew. Chem., Int. Ed.*, 2005, **44**, 5187.
- 11 (a) A. K. Bar, C. Pichon, N. Gogoi, C. Duhayon, S. Ramasesha and J. P. Sutter, *Chem. Commun.*, 2015, **51**, 3616; (b) R. Ruamps, L. J. Batchelor, R. Maurice, N. Gogoi, J. L. Pablo, N. Guihry, C. Graaf, A. L. Barra, J. P. Sutter and T. Mallah, *Chem. -Eur. J.*, 2013, **19**, 950.
- 12 (a) Y. -Z. Zhang, B. -W. Wang, O. Sato, S. Gao, *Chem. Commun.* 2010, **46**, 6959; (b) T. S. Venkatakrishnan, S. Sahoo, N. Bréfuel, C. Paulsen, C. Duhayon, A. L. Barra, S. Ramasesha and J. P. Sutter, *J. Am. Chem. Soc.*, 2010, **132**, 6047.
- 13 S. M. Nelson, P. D. A. McIlroy, C. S. Stevenson, E. König, G. Ritter and J. Waigel, *J. Chem. Soc., Dalton Trans.*, 1986, 991.
- 14 *SAINT Software Users Guide*, version 7.0; Bruker Analytical XRay Systems: Madison, WI, 1999.
- 15 Sheldrick, G. M. *SADABS*, version 2.03; Bruker Analytical X-Ray Systems, Madison, WI, 2000.
- 16 Sheldrick, G. M. *SHELXTL*, Version 6.14, Bruker AXS, Inc.; Madison, WI 2000-2003.
- 17 M. Llunell, D. Casanova, J. Cirera, P. Alemany and S. Alvarez, *SHAPE*, Version 2.1. Universitat de Barcelona, 2013.
- 18 N. F. Chilton, R. P. Anderson, L. D. Turner, A. Soncini, K. S. Murray, *J. Comput. Chem.*, 2013, **34**, 1164.
- 19 M. P. Shores, J. J. Sokol and J. R. Long, *J. Am. Chem. Soc.*, 2002, **124**, 2279.
- 20 S. Gomez-Coca, E. Cremades, N. Aliaga-Alcalde, E. Ruiz, *J. Am. Chem. Soc.* 2013, **135**, 7010.
- 21 (a) A. V. Pali, O. S. Reu, S. M. Ostrovsky, S. I. Klokishner, B. S. Tsukerblat, Z.-M. Sun, J.-G. Mao, A. V. Prosvirin, H.-H. Zhao and Kim R. Dunbar, *J. Am. Chem. Soc.*, 2008, **130**, 14729; (b) K. Bernot, J. Luzon, R. Sessoli, A. Vindigni, J. Thion, S. Richeter, D. Leclercq, J. Larionova, and A. Lee, *J. Am. Chem. Soc.*, 2008, **130**, 1619; (c) H.-L. Sun, Z.-M. Wang and S. Gao, *Chem. -Eur. J.*, 2009, **15**, 1757.
- 22 J. A. Mydosh, *Spin Glasses : An Experimental Introduction*, Taylor & Francis, London, 1993.
- 23 K. S. Cole and R. H. Cole, *J. Chem. Phys.*, 1941, **9**, 341.
- 24 S. M. Aubin, Z. Sun, L. Pardi, J. Krzysteck, K. Folting, L. J. Brunel, A. L. Rheingold and D. N. Hendrickson, *Inorg. Chem.*, 1999, **38**, 5329.